

Parameter Estimation for Simultaneous Saccharification and Fermentation of Food Waste Into Ethanol Using Matlab Simulink

Rebecca Anne Davis

Received: 15 May 2007 / Accepted: 4 September 2007 /

Published online: 6 October 2007

© Humana Press Inc. 2007

Abstract The increase in waste disposal and energy costs has provided an incentive to convert carbohydrate-rich food waste streams into fuel. For example, dining halls and restaurants discard foods that require tipping fees for removal. An effective use of food waste may be the enzymatic hydrolysis of the waste to simple sugars and fermentation of the sugars to ethanol. As these wastes have complex compositions which may change day-to-day, experiments were carried out to test fermentability of two different types of food waste at 27° C using *Saccharomyces cerevisiae* yeast (ATCC4124) and Genencor's STARGENT™ enzyme in batch simultaneous saccharification and fermentation (SSF) experiments. A mathematical model of SSF based on experimentally matched rate equations for enzyme hydrolysis and yeast fermentation was developed in Matlab Simulink®. Using Simulink® parameter estimation 1.1.3, parameters for hydrolysis and fermentation were estimated through modified Michaelis–Menten and Monod-type equations with the aim of predicting changes in the levels of ethanol and glycerol from different initial concentrations of glucose, fructose, maltose, and starch. The model predictions and experimental observations agree reasonably well for the two food waste streams and a third validation dataset. The approach of using Simulink® as a dynamic visual model for SSF represents a simple method which can be applied to a variety of biological pathways and may be very useful for systems approaches in metabolic engineering in the future.

Keywords Food waste · Hydrolysis · Ethanol · Simultaneous saccharification and fermentation · Matlab · Simulink® · Parameter estimation · Metabolic engineering

R. A. Davis (✉)

Department of Agricultural & Biological Engineering, Purdue University, 225 South University Street,
West Lafayette, IN 47907-2093, USA
e-mail: davis160@purdue.edu

Nomenclature

C_{etoh}	ethanol concentration (g/l)
C_{fru}	fructose concentration (g/l)
C_{glc}	glucose concentration (g/l)
C_{gly}	glycerol concentration (g/l)
C_{mal}	maltose concentration (g/l)
C^{in}	inhibitory product concentration (g/l)
C_{starch}	starch concentration (g/l)
C_{suc}	sucrose concentration (g/l)
$C_{x,0}$	initial concentration (x =component g/l)
K_i	competitive inhibition constant (g/l)
K_m	Michaelis–Menten constant (g/l)
K_s	uncompetitive inhibition constant of starch (g/l)
N	toxic power constant for glucose product inhibition
PME	processed ready-to-eat food
RICE	rice mixture
SSF	simultaneous saccharification and fermentation
V_m	maximal initial reaction rate ($\text{g l}^{-1} \text{h}^{-1}$)
Y_{el}	fraction of glucose to ethanol ($1 - Y_{\text{el}}$ =fraction to glycerol)
$Y_{\text{glc/mal}}$	yield of glucose to maltose
$Y_{\text{glc/starch}}$	yield of glucose to starch
$Y_{\text{hex/suc}}$	yield of hexose to sucrose
$Y_{\text{etoh/hex}}$	yield of ethanol to hexose
$Y_{\text{gly/hex}}$	yield of glycerol to hexose

Introduction

In the USA alone, more than 91 billion pounds of edible food (27% of what is produced for consumption) are lost each year by the retail, consumer, and food service industries, almost all of which is unrecoverable [1]. Composting is one recovery path; however, it is time-consuming, location-dependent, and subject to contamination. At Purdue University, food waste from cafeteria trays is discarded separately from other trash and accounts for approximately 150 tons of food waste from residence halls and the Union. This does not include the waste from food prep. It is estimated that 340 tons per year of food waste is thrown in dumpsters or trash bins on Purdue campus (J. Zarate, West Lafayette, IN, 2006, personal communication).

A mobile or stand-alone unit which would controllably convert food waste into ethanol at a busy cafeteria or restaurant would be attractive if the economics were favorable. Using a black-box model, several components are considered important for monitoring the conversion into ethanol (Fig. 1).

Preliminary experiments determined that a loading of 0.8 g STARGENTTM enzyme (mixture of alpha-amylase and glucoamylase) and 90 g pre-grown *Saccharomyces cerevisiae* (ATCC4124) per liter of food waste slurry was sufficient. Under these conditions, hydrolysis and fermentation rates were not dependent on mass transfer limitations up to the maximum food waste slurry concentration of 400 g/l solids (104 g/l starch, 136 g/l mono- and disaccharides). To determine the final concentrations of ethanol and glycerol from initial concentrations of sugars and starch, datasets for hydrolysis and simultaneous saccharification and fermentation (SSF) of two types of food waste were used as fitting criteria for nonlinear

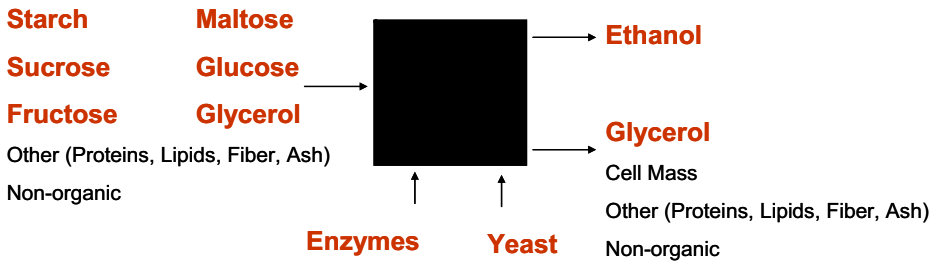


Fig. 1 The black-box model showing relevant inputs and outputs for SSF conversion of food waste

parameter estimation of kinetic model parameters. The kinetic models were based on established Michaelis–Menten and Monod-type equations.

The objective of this study was to generate a simple, editable, SSF black-box model template which could predict ethanol and glycerol production based on initial food waste conditions. With increased datasets and more advanced mathematical functions, these models and their predictive ability will continue to improve. The heterogeneous nature of food waste requires a robust model which can handle changing feed composition. These models, once improved, could serve as predictive tools to determine the expected ethanol productivity per year to control flow rates on a mobile unit or to determine the economic drivers of such a system.

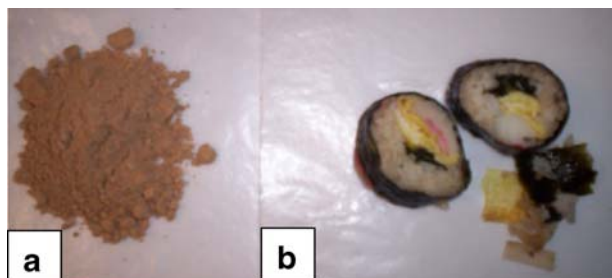
Materials and Methods

Food Material

Two samples of homogenized food waste were used to match hydrolysis and SSF fermentation profiles to the kinetic models. The first sample was a mixture of processed ready-to-eat packaged food (PRE). LC analysis matched the composition of simple sugars and glycerol found on the PRE packages. Additional nutritional data on packages was used to determine starch (by difference), protein, ash, and lipids content. Theoretical ethanol yield for the PRE sample at a concentration of 100 g/l was 32.0 g/l.

The second food sample was a rice mixture which contained seaweed, egg, rice, imitation crab, and spinach. LC analysis was used to determine sugars and glycerol. Relative moisture, protein, lipid, ash, and carbohydrates were calculated based on USDA National Nutrient Database [2]. Theoretical ethanol yield for a 100 g/l sample was 34.6 g/l. Pictures of the dried, homogenized PRE mixture and the rice mixture are shown in Fig. 2a and b, respectively. Compositions of the two food mixtures are seen in Fig. 3. The PRE mixture (Fig. 3a) has less

Fig. 2 Food waste (a) dried, homogenized PRE mixture (b) rice mixture



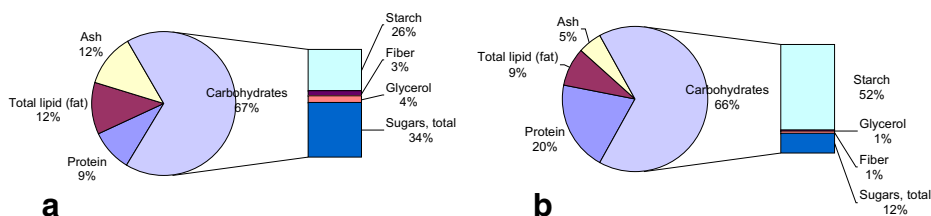


Fig. 3 Food waste composition on dry basis (a) PRE mixture (b) rice mixture

starch and more sugars (mono- and disaccharides), but the same overall composition of carbohydrates compared to the rice mixture (Fig. 3b).

A third set of data was prepared to represent a typical kitchen waste stream (food, plastic, paper, cardboard, etc.). Initial composition of the validation dataset was $C_{\text{starch}} = 25 \text{ g/l}$, $C_{\text{glc}} = 5.7 \text{ g/l}$, $C_{\text{mal}} = 2.9 \text{ g/l}$, $C_{\text{suc}} = 1 \text{ g/l}$, $C_{\text{fru}} = 7.8 \text{ g/l}$, $C_{\text{gly}} = 1.2 \text{ g/l}$. This mixture was run under both hydrolysis only, and SSF conditions and the models created from the PRE and Rice mixture samples were compared as predictive models to the validation dataset. The PRE, Rice, and validation mixtures all had pH values of around pH=7 at 100 g/l concentration. The pH was not controlled throughout hydrolysis and SSF to mimic the simplest design scenario and lessen the model complexity.

Hydrolysis Procedure

Hydrolysis experiments were carried out in a G-24 Environmental Incubator (New Brunswick Scientific, Edison, NJ, USA) set on 250 rpm. Hydrolysis vessels were a 300-ml Erlenmeyer flask with sidearm sealed as in SSF experiments to allow identical conditions to SSF. The hydrolysis experiments were run at 27 °C (the optimal yeast growth temperature) to match the SSF experiments. The recommended conditions for STARGENTM enzyme is between 20 and 40 °C.

The food slurry was allowed to shake for 1–5 min before STARGENTM enzyme was added. Samples were taken in 1-ml volumes and pipetted into Optimum Tubes (Life Science, Colorado, USA). If the mixture was especially viscous or large pieces of matter were present, the pipette tips were cut to prevent clogging. The hydrolysis was ended by immediately spinning down samples in an Eppendorf centrifuge at RT for 5 min and 12,000 rpm then filtering the supernatant using a 3-ml syringe with Luer-Lok (Beckton Dickinson, NJ, USA) and 25-mm, 0.2- μm syringe filter (Fisher Scientific). The filtrate was stored in the freezer for future analysis.

SSF Procedure

SSF experiments were performed in a 300-ml Erlenmeyer flask with sidearm at 27 °C and 250 rpm. Yeast was pre-grown in 100 ml YEPD overnight until reaching 500–550 KU (~90 g/l), spun down, and then added to the food waste mixture. STARGENTM enzyme was added, and the flasks were sealed with Saran wrap to allow fermentation to be carried out under largely anaerobic conditions. Figure 4 shows the two mixtures undergoing SSF.

Analytical Methods

LC columns were used to measure the simple sugars, glycerol, and ethanol. For monosaccharides, a YMC-Pack PolyamineII column (4.6×250 mm; Japan) with column

Fig. 4 Batch SSF experiments of food waste



heater (25 °C) was used, with an autoinjector (Hitachi AS-4000), pump (Hitachi L-6200), RI detector (Hitachi L-3350), and a computing integrator (Hitachi D-2500) at 40- μ l injection volumes. The mobile phase was 75/25 Acetonitrile/DIW, degassed and filtered through a 0.2- μ m nylon filter (Millipore).

For maltose, ethanol, and glycerol, an Aminex HPX-87H ion exchange column (Biorad, Hercules, CA, USA) with column heater (50 °C) was used with a Varian 9010 Solvent Delivery System, Waters 717plus Autosampler, Waters 2414 refractive index detector, and a Hewlett Packard HP3396G integrator at 50- μ l injection volumes. The mobile phase was degassed 5 mM H_2SO_4 and filtered through a 0.2- μ m nylon filter (Millipore).

Mathematical Models

Model Structure

The experimental and mathematical models were divided into two hierarchical steps, as seen in Fig. 5. First, hydrolysis experiments were conducted, and the hydrolysis time profile was matched to hydrolysis rate equations. A separate hydrolysis-only model was used to match the hydrolysis data to Michaelis–Menten based kinetics and to solve for unknown parameters. Second, SSF experiments were conducted using identical enzyme loading, and these datasets were matched to a complete SSF model. The SSF model incorporated the hydrolysis parameters from the first step and was used to solve for the unknown fermentation parameters using Monod-based kinetics.

Fig. 5 Decomposition of hydrolysis and SSF models

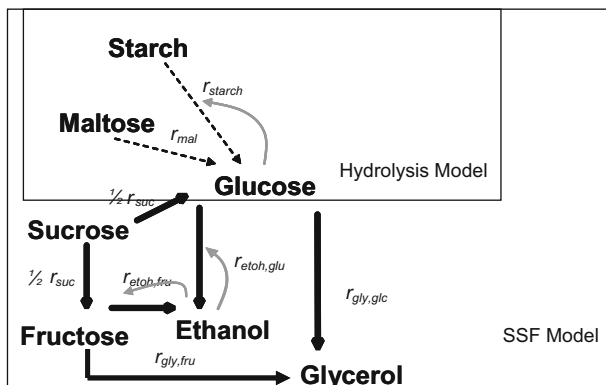


Table 1 Balance equations for the hydrolysis model.

Hydrolysis model

$$\begin{aligned}\frac{dC_{\text{starch}}}{dt} &= -r_{\text{starch}} \\ \frac{dC_{\text{mal}}}{dt} &= -r_{\text{mal}} \\ \frac{dC_{\text{glc}}}{dt} &= Y_{\text{glc/mal}}r_{\text{mal}} + Y_{\text{glc/starch}}r_{\text{starch}}\end{aligned}$$

Tables 1 and 2 list the complete set of mass balance equations for the hydrolysis model and the SSF model. Dilution due to cell growth was not included in the model, nor was a cell mass balance. As cells were grown to maximal exponential phase before the batch runs and the fermentation was 90% complete in 5 h or less, any maintenance or growth requirements were neglected, and yield coefficients were used to determine the conversion yield for each reaction rate.

Simulink Model

The Matlab Simulink® Model was designed to represent the model structure and mass balance equations for SSF and is shown in Fig. 6. Shaded boxes represent the reaction rates, which have been lumped into subsystems. To solve the system of ordinary differential equations (ODEs) and to estimate unknown parameters in the reaction rate equations, the interface parameter estimation was used. This program allows the user to decide which parameters to estimate and which type of ODE solver and optimization technique to use. The user imports observed data as it relates to the input, output, or state data of the Simulink® model. With the imported data as reference, the user can select options for the ODE solver (fixed step/variable step, stiff/non-stiff, tolerance, step size) as well options for the optimization technique (nonlinear least squares/simplex, maximum number of iterations, and tolerance). With the selected solver and optimization method, the unknown independent, dependent, and/or initial state parameters in the model are determined within set ranges. For this study, nonlinear least squares regression was used with Matlab ode45, which is a Runge–Kutta [3, 4] formula for non-stiff systems. The steps of nonlinear least squares regression are as follows:

1. Guess initial values for parameters: K_{mm} , V_{mm} , K_{ms} , $Y_{\text{Glc/S}}$, etc. Set $n(\text{iteration})=0$.
2. Solve for $dy(t)/dt$ using Simulink simulation and iterative solver (ode45).
3. Use optimization algorithm to update parameters (nonlinear least square).
4. Check if minimization is reached $|J^{n+1}-J^n| < \text{tolerance}$. If not, set $n=n+1$ and go back to step 2 for next iteration.

Table 2 Balance equations for the SSF model.

SSF model

$$\begin{aligned}\frac{dC_{\text{starch}}}{dt} &= -r_{\text{starch}} \\ \frac{dC_{\text{mal}}}{dt} &= -r_{\text{mal}} \\ \frac{dC_{\text{glc}}}{dt} &= Y_{\text{glc/mal}}r_{\text{mal}} + Y_{\text{glc/starch}}r_{\text{starch}} + \frac{1}{2}Y_{\text{hex/suc}}r_{\text{suc}} \\ &\quad - r_{\text{etoh,glc}} - r_{\text{gly,glc}} \\ \frac{dC_{\text{suc}}}{dt} &= -r_{\text{suc}} \\ \frac{dC_{\text{fru}}}{dt} &= \frac{1}{2}Y_{\text{hex/suc}}r_{\text{suc}} - r_{\text{etoh,fru}} - r_{\text{gly,fru}} \\ \frac{dC_{\text{etoh}}}{dt} &= Y_{\text{el}}[Y_{\text{etoh/hex}}(r_{\text{etoh,glc}} + r_{\text{etoh,fru}})] \\ \frac{dC_{\text{gly}}}{dt} &= (1 - Y_{\text{el}})[Y_{\text{gly/hex}}(r_{\text{gly,glc}} + r_{\text{gly,fru}})]\end{aligned}$$

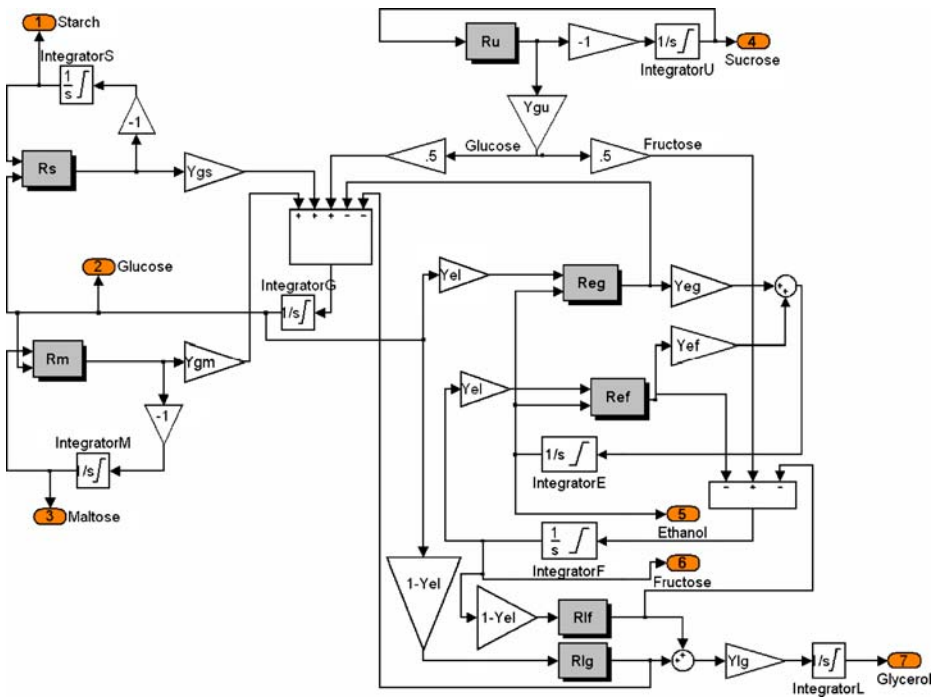


Fig. 6 Matlab Simulink model for SSF parameter estimation

The cost function, J , is a calculation of the squared errors for the two models to the datasets. If the minimization between the model-simulated results for each of the cases results in exactly the same system parameters, the cost function will be driven to zero.

Kinetic Rate Equations

Table 3 lists the kinetic rate expressions for each of the hydrolysis and fermentation reaction rates shown in Fig. 5 and in the mass balance equations of Tables 1 and 2. Each of the reaction rates were found to fit the data through trial and error, starting with the simplest model. For the hydrolysis reaction rates (r_{starch} and r_{maltose}), the simplest form was the Michaelis–Menten model without inhibition. For all other reaction rates which described fermentation kinetics, the simplest form was the Monod model without inhibition. More descriptive models were found in the literature and tested one by one until the set of kinetic rate equations with the best fit to the experimental data were determined. This was completed with the hydrolysis datasets first, then the complete SSF datasets.

The reaction rate for the hydrolysis of starch (Eq. 2.1 in Table 3) is a Michaelis–Menten type model, which considers competitive product inhibition of glucose and substrate inhibition of starch. The hydrolysis of maltose (Eq. 2.2 in Table 3) is represented by a Michaelis–Menten type model with competitive product inhibition. These equations were tested by Lopez et al. [3] for hydrolysis of chestnut puree by an alpha and glucoamylase mixture. As the enzyme STARGENT™ also contains amounts of alpha and glucoamylase, it was not surprising that they (Eqs. 2.1–2.2 in Table 3) fit the hydrolysis data better than non-inhibitory Michaelis–Menten kinetics.

Table 3 Kinetic rate equations.

Equations	Number	Reference
$r_{\text{starch}} = \frac{C_{\text{starch}} V_{m,\text{starch}}}{C_{\text{starch}} + K_{m,\text{starch}} \left(\frac{C_{\text{glc}}}{K_{i,\text{starch}}} + 1 \right) + K_{s,\text{starch}} C_{\text{starch}}^2}$	(2.1)	[4]
$r_{\text{mal}} = \frac{C_{\text{mal}} V_{m,\text{mal}}}{C_{\text{mal}} + K_{m,\text{mal}} \left(\frac{C_{\text{glc}}}{K_{i,\text{mal}}} + 1 \right)}$	(2.2)	[4]
$r_{\text{suc}} = \frac{C_{\text{suc}} V_{m,\text{suc}}}{C_{\text{suc}} + K_{m,\text{suc}}}$	(2.3)	
$r_{\text{etoh,glc}} = \frac{-C_{\text{glc}} V_{m,\text{glc}}}{C_{\text{glc}} + K_{m,\text{glc}}} \left(1 + \frac{C_{\text{etoh}}}{C_{\text{etoh}}^M} \right)^n$	(2.4)	[7]
$r_{\text{etoh,fru}} = \frac{-C_{\text{fru}} V_{m,\text{fru}}}{C_{\text{fru}} + K_{m,\text{fru}}} \left(1 + \frac{C_{\text{etoh}}}{C_{\text{etoh}}^M} \right)^n$	(2.5)	[7]
$r_{\text{gly,glc}} = \frac{C_{\text{glc}} V_{m,\text{gly}}}{C_{\text{glc}} + K_{m,\text{gly}}}$	(2.6)	
$r_{\text{gly,fru}} = \frac{C_{\text{fru}} V_{m,\text{gly}}}{C_{\text{fru}} + K_{m,\text{gly}}}$	(2.7)	

For the fermentation reaction kinetics, both the sucrose (Eq. 2.3 in Table 3) and glycerol reactions (Eqs. 2.6–2.7 in Table 3) used were simple Monod models without inhibition. Sucrose is hydrolyzed by invertase, an enzyme in the yeast cell envelope. When glucose levels are high, the invertase repressor genes are expressed, and when low, the expression is derepressed [4]. For sucrose, therefore, the hydrolysis into fructose and glucose is dependent on the concentration of glucose and is purely enzymatic; the sucrose molecule is not transported into the yeast cell. It is unclear at what concentration of glucose the invertase expression is repressed and whether the conversion is inhibited by either glucose or fructose. For simplicity, a simple Monod equation was used and found to fit the data well, with cost functions lower than modified Monod equations.

Glycerol formation is another pathway besides ethanol formation to replenish NAD^+ and maintain redox balance in the cell. In addition, glycerol is important for osmoregulation where,

Table 4 Hydrolysis initial and kinetic parameters.

	100 g/l PRE	400 g/l PRE	Units
Initial conditions			
$C_{\text{starch},0}$	26.1	104	g/l
$C_{\text{mal},0}$	3.33	13.3	g/l
$C_{\text{glc},0}$	5.42	21.7	g/l
$C_{\text{suc},0}$	20.0	80.0	g/l
$C_{\text{fru},0}$	5.04	20.2	g/l
Evaluated parameters			
$V_{m,\text{starch}}$	417		$\text{g l}^{-1} \text{h}^{-1}$
$K_{m,\text{starch}}$	27		g/l
$K_{i,\text{starch}}$	0.5		g/l
$K_{s,\text{starch}}$	0.076		g/l
$V_{m,\text{mal}}$	343		$\text{g l}^{-1} \text{h}^{-1}$
$K_{m,\text{mal}}$	4.97		g/l
$K_{i,\text{mal}}$	0.77		g/l
$Y_{\text{glc/starch}}$	0.66		
$Y_{\text{glc/mal}}$	1.05		

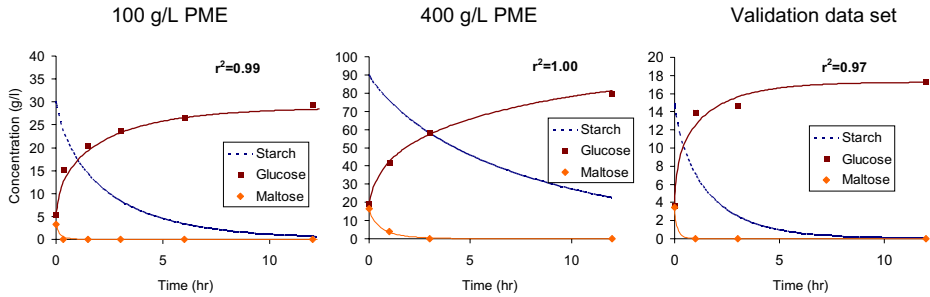


Fig. 7 Comparison of measured to simulated data for the hydrolysis experiments using the PRE mixture at 100, 400 g/l, and the validation data set

under conditions of decreased extracellular water activity, glycerol formation is increased [5]. Glycerol is produced at the expense of ethanol production and, after trial-and-error with product inhibition models, the simple Monod model gave best fits to the data based on the lowest resulting cost function.

Table 5 SSF initial and kinetic parameters.

	100 g/l PRE	100 g/l rice mixture	Units
Initial conditions			
$C_{\text{starch},0}$	26.1	52.5	g/l
$C_{\text{mal},0}$	3.33	0.66	g/l
$C_{\text{glc},0}$	5.42	4.04	g/l
$C_{\text{suc},0}$	20.0	3.090	g/l
$C_{\text{fru},0}$	5.04	4.05	g/l
Fixed parameters			
$V_{m,\text{starch}}$	417		$\text{g l}^{-1} \text{h}^{-1}$
$K_{m,\text{starch}}$	27		g/l
$K_{i,\text{starch}}$	0.5		g/l
$K_{s,\text{starch}}$	0.076		g/l
$V_{m,\text{mal}}$	343		$\text{g l}^{-1} \text{h}^{-1}$
$K_{m,\text{mal}}$	4.97		g/l
$K_{i,\text{mal}}$	0.77		g/l
$Y_{\text{glc}/\text{starch}}$	0.66		
$Y_{\text{glc}/\text{mal}}$	1.05		
N	0.36		
$Y_{\text{hex}/\text{suc}}$	1.05		
C_{etoh}	100		g/l
$K_{m,\text{glc}}=K_{m,\text{fru}}$	0.315		g/l
Evaluated parameters			
$V_{m,\text{suc}}$	14.5		$\text{g l}^{-1} \text{h}^{-1}$
$K_{m,\text{suc}}$	2.7		g/l
$V_{m,\text{glc}}$	15		$\text{g l}^{-1} \text{h}^{-1}$
$V_{m,\text{fru}}$	4.2		$\text{g l}^{-1} \text{h}^{-1}$
$V_{m,\text{gly}}$	45.1		$\text{g l}^{-1} \text{h}^{-1}$
$K_{m,\text{gly}}$	101		g/l
$Y_{\text{gly}/\text{hex}}$	1.02		
Y_{el}	0.81		
$Y_{\text{etoh}/\text{hex}}$	0.511		

The utilization of glucose and fructose into ethanol uses the Levenspiel toxic inhibition equation for ethanol production [6]. This was used after more complex rate expressions including both substrate and product inhibition failed to improve model performance evidenced by failing to decrease the cost function.

Results and Discussion

Hydrolysis Results

Parameter estimate results from best fit kinetic expressions are listed in Table 4 for each of the hydrolysis reaction rates and yield coefficients. Using these parameters, Fig. 7 compares measured to simulated data for the hydrolysis experiments using the MRE mixture at 100, 400 g/l, and the validation dataset. The r^2 values, coefficient of determination, for glucose are 0.99, 1.00, 0.97, respectively, indicating a good fit to all three datasets.

SSF Results

The SSF parameters are listed in Table 5 and the measured and calculated data can be seen in Fig. 8. In modeling the fermentation reaction kinetics, it was found that for the parameter estimation simulations to match Matlab Simulink® simulations of the same model, the data had to be weighted. Giving higher weights to a data point means that the selected data point has more influence over the parameter estimates. If certain data points are more precisely

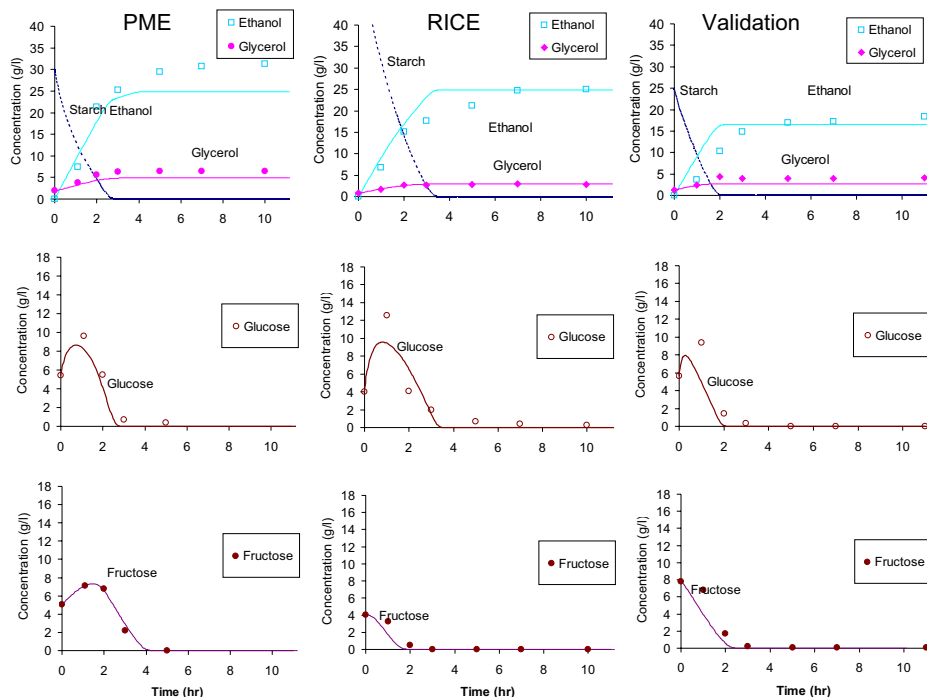


Fig. 8 Measured and simulated data for the SSF experiments using the PME mixture, the RICE mixture, and the validation data set

measured, for instance, then they should be given higher weighting than the points which are not precisely measured [7]. In the case of SSF, all but two trends (glucose and fructose) followed either an increasing or decreasing pattern. Given equal weighting, this meant that the optimization technique estimated the same, regardless of these two trends behaving differently (stiffer) than the other trends. The result of weighting the same led to what appeared to be converging solutions on the parameter estimation screen; however, there was misalignment of the glucose and fructose profiles. Giving higher weight to the measurements which change faster (and thus represent higher precision due to faster changing values than the other trends) gave the results in Table 5 using the following weighting factors: glucose and fructose (2), glycerol and ethanol (0.2), and maltose and sucrose (0.1).

Design

To determine a rough productivity evaluation, the validation dataset used in the models was made to represent a typical kitchen waste stream (food, plastic, paper, cardboard, etc.) Despite being mixed with other waste materials, the validation dataset fit the hydrolysis and SSF models well. If all Purdue food waste was at the concentrations in the SSF validation set and a stand-alone system converted food waste at the same yield, then 340 tons of food waste could be converted into 73 tons=146,000 lbs=22,500 gallons ethanol. The capital equipment would be quite high, making it difficult to achieve a short payback period. Energy required for ethanol separation and grinding is another factor, although electricity and heat may be provided cheaply if non-fermentable solids are thermochemically treated. More work needs to be done to analyze the economic feasibility of converting food waste to ethanol.

Conclusion

Hydrolysis and fermentation models were developed using two hydrolysis datasets and two SSF datasets and by using modified Michaelis–Menten and Monod-type kinetics. Validation experiments made to represent typical kitchen waste correlated well with both models. The models were generated in Matlab Simulink® and represent a simple method for implementing ODE system solvers and parameter estimation tools. These types of visual dynamic models may be useful for applying kinetic or linear-based metabolic engineering of bioconversion processes in the future.

Acknowledgements We would like to thank Defense Life Sciences (McLean, VA) and Purdue Agricultural Research Programs for funding for this project and Genencor International for providing enzymes. Also thanks to Dr. Michael Ladisch, Dr. Nathan Mosier, and Dr. Miroslav Sedlak for their advice and help in many aspects of this project.

References

1. Kantor, L. S., & Lipton, K. (1997). *Food Review*, 20(1), 2–12.
2. USDA National Nutrient Database for Standard Reference. Retrieved September 2005 from <http://www.nal.usda.gov/fnic/foodcomp/search/>.
3. Lopez, C., Tarrado A., et al. (2006). *Enzyme and Microbial Technology*, 39(2), 252–258.
4. Walker, G. M. (1998). *Yeast physiology and biotechnology*. New York: Wiley.
5. Wang, Z. X., Zhuge, J., et al. (2001). *Biotechnology Advances*, 19, 201–223.
6. Levenspiel, O. (1980). *Biotechnology and Bioengineering*, 22, 1671–1687.
7. Handbook of Statistical Methods. Retrieved Jun 2006 from <http://www.itl.nist.gov/div898/handbook/>.